

Comparative Study on the Optimization Methods for a Motor Drive of Artificial Hearts

André Pohlmann[†], Marc Leßmann* and Kay Hameyer*

Abstract – Worldwide cardiovascular diseases are the major cause of death. Aside from heart transplants, which are limited due to the availability of human donor hearts, artificial hearts are the only therapy available for terminal heart diseases. For various reasons, a total implantable artificial heart is desirable. But the limited space in the human thorax sets rigorous restrictions on the weight and dimensions of the device. Nevertheless, the appropriate functionality of the artificial heart must be ensured and blood damage must be prevented. These requirements set further restrictions to the drive of this device. In this paper, two optimization methods, namely, the manual parameter variation and Differential Evolution algorithm, are presented and applied to match the specifications of an artificial heart.

Keywords: Artificial hearts, Differential evolution, Finite-element method (FEM), Linear drives, Optimization

1. Introduction

Heart transplants are a limited option for treating heart diseases. Thus, artificial hearts are necessary. Currently, CardioWest is the only clinically approved total artificial heart (TAH) system worldwide. In order to avoid its drivelines through the human abdominal wall, it is desirable to completely implant a TAH in the human thorax. This will improve the patient's quality of life and reduce the risk of infection. However, the limited space in the thorax restricts the weight and dimensions of an implantable artificial heart and its drive. Nevertheless, the drive has to provide the required force for the pump to achieve a sufficient perfusion of the human body. The resulting losses of the blood pump must be limited to prevent blood damage due to overheating.

Fig. 1(a) shows the bisection of the drive of a pulsatile artificial heart developed at the Institute of Electrical Machines at RWTH Aachen University. Two optimization methods for the drive are studied in this paper. The drive is excited by an inner and an outer permanent-magnet ring made of neodymium iron boron (NdFeB). Compared to the remanent induction $B_{r(in)}$ of the inner magnet ring, which is 1.44 T, the remanent induction $B_{r(out)}$ of the outer magnet ring only averages to 1.35 T. Pole shoes are attached above and under the magnets to concentrate the induction in the air gap. They are made of an iron vanadium cobalt alloy (referred in this paper by its commercial name Vacoflux), which has a saturation induction of 2.4 T. The mover consists of four coils. Each

coil is hand wound with a rectangular copper wire. By this way, a copper fill factor of 75% is achieved. In Fig. 1(b), the magnetization of the magnets and the flux path are indicated by arrows. When supplying the coils with a direct current, the direction of the coil movement can be determined by applying the Lorentz force Eq. (1). The drive weighs 616 g. During the simulation, the electrical losses occurring in the drive were calculated to 8 W, when providing the required force (Fig. 2) for the blood pump to generate a sufficient perfusion of the body. As the medium aortic pressure of 100 mmHg is much higher than the pressure in the pulmonary blood circuit, which is 27 mmHg, the absolute value of the required forces for pumping blood in the left blood circuit is much higher than the required ones for the right blood circuit.

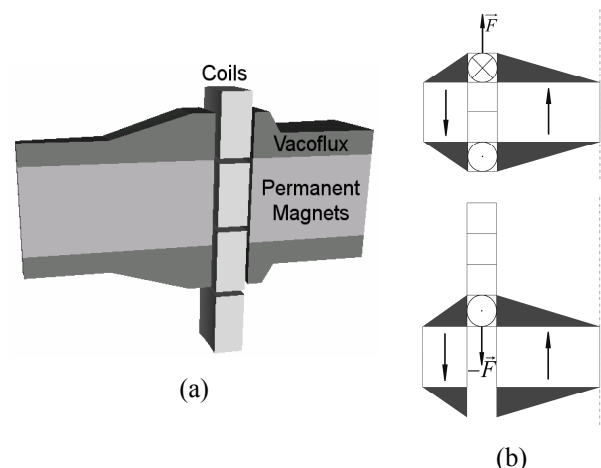


Fig. 1. Drive of an artificial heart.

[†] Corresponding Author: Institute of Electrical Machines, RWTH Aachen University, Germany (Andre.Pohlmann@iem.rwth-aachen.de)

* Institute of Electrical Machines, RWTH Aachen University, Germany
Received: December 31, 2010; Accepted: October 13, 2011

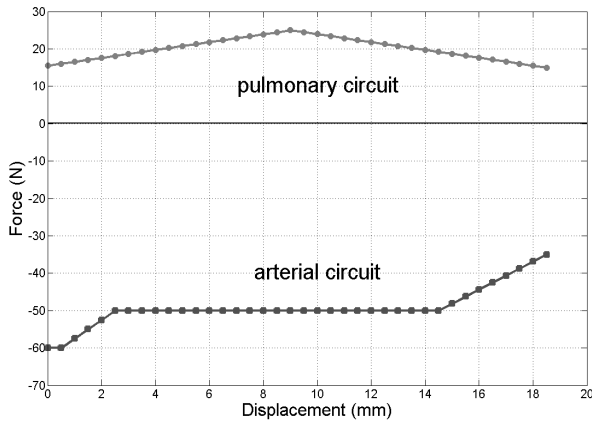


Fig. 2. Force versus displacement characteristic.

2. Optimization chain

Both of the optimization methods, which will be introduced in the next section, follow an optimization chain consisting of three steps. Based on the input parameters, the mesh required for the finite-element method (FEM) simulation of the induction distribution in the drive’s air gap is generated. Finally, the weight and the losses of the modeled drive are analytically calculated. Based on the required forces, the optimal current supply of the coils, depending on the air gap induction, is determined to achieve a good efficiency.

2.1 Input parameters

The optimization process is automated by establishing a parameterizable computer model for the mesh generation. As shown in Fig. 3, the model is defined by five fixed parameters (*a* to *e*) and seven variable parameters. A parameter file is created that can automatically initialize the variables required for the generation of the computer models and their meshes.

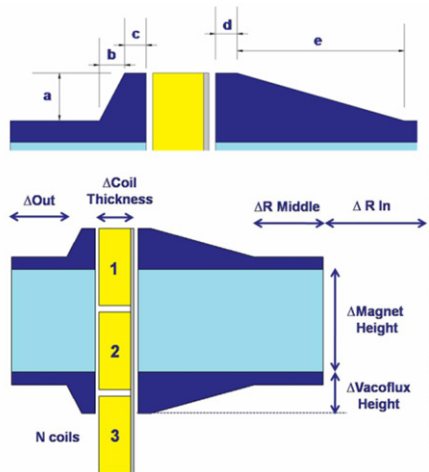


Fig. 3. Parameterized drive for optimization.

2.2 FEM simulation

The position-dependent driving force $\vec{F}_n(x)$ of the actuator can be calculated using the Lorentz force equation

$$\vec{F}_n(x) = I_n(x) \cdot (\vec{l} \times \vec{B}_n(x)) \quad (1)$$

Aside from the active wire length of the coils *l* and the coil supply $I_n(x)$, the radial induction distribution $\vec{B}_{r,n}(x)$ in the air gap is required to determine the force output. Its direction is dependent on the coil supply, as shown in Fig. 1(b). Considering that the magnetic leakage flux is significant and the iron vanadium cobalt alloy is magnetically saturated (Fig. 4), nonlinear FEM simulations, which are performed using a 3-D static problem solver from the in-house FE software package iMoose of the Institute of Electrical Machines 0, are employed to determine the induction.

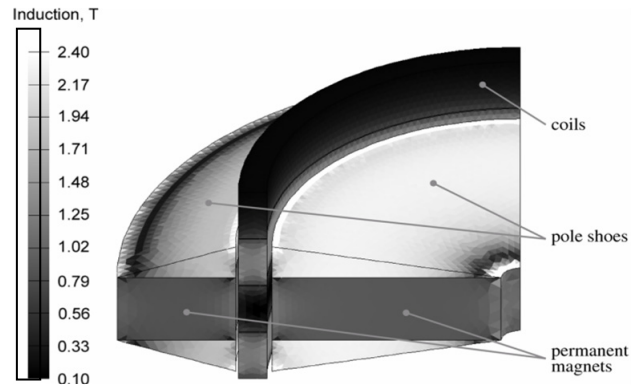


Fig. 4. Induction distribution in the drive.

2.3 Calculation of weight and losses

The weight and resulting losses have to be computed for the optimization process. Although the total weight of the drive can be calculated by multiplying the volumes (extracted from CAD models) by their material densities and adding the resulting weights, a calculation chain is required to determine the resulting losses. The counter effects of the field excited by the coils can be neglected because of the 4 mm air gap width between the inner and outer permanent-magnet rings. Moreover, the iron losses in the pole shoes and permanent magnets are negligible in the operation frequency range between 1.33 and 2.66 Hz. Hence, the ohmic losses of each coil are dominant. The coils should be supplied depending on the average radial magnetic field distribution $\vec{B}_{r,n}(x)$ penetrating each coil *n* at displacement *x* in the air gap to keep the losses as low as possible. Therefore, the current factors $k_{r,n}(x)$ are calculated by evaluating the induction distribution obtained by the previous FEM simulations for each coil and position *x* of the axial displacement

$$k_{I,n}(x) = \frac{\bar{B}_{r,n}(x)}{\sum_{n=1}^4 |\bar{B}_{r,n}(x)|}. \quad (2)$$

Before the current supply $I_{n,fw/bw}(x)$ for each coil can be calculated using

$$I_{n,fw/bw}(x) = k_{I,n}(x) \cdot I_{sum,fw,bw}(x), \quad (3)$$

the current value $I_{sum,fw,bw}(x)$ has to be determined first.

Therefore, the Lorentz force Eq. (1) is transformed into

$$I_{sum,fw/bw}(x) = \frac{F_{required,fw/bw}(x)}{\sum_{n=1}^4 \bar{B}_{r,n}(x) \cdot k_{I,n}(x) \cdot l}. \quad (4)$$

The force $F_{required,fw/bw}(x)$ required for the blood pump can be obtained from Fig. 2. Considering that the forces for the pulmonary and arterial blood circuits differ, the annotations fw (pulmonary) and bw (arterial) are used to indicate the direction of the coil movements. Finally, the resulting ohmic losses $P_{sum,fw/bw}(x)$ are determined by adding the ohmic losses of each coil. Each loss can be determined by multiplying the square of the coil's current $I_{n,fw/bw}(x)$ with the winding resistance R

$$P_{sum,fw/bw}(x) = \sum_{n=1}^4 I_{n,fw/bw}^2(x) \cdot R. \quad (5)$$

In order to compute the average losses during one beat cycle, the maximum axial displacement of the pusher plates of 18.5 mm is divided into segments with a length of 0.5 mm

$$x_m = m \cdot 0.5 \text{ mm}, \quad m = 0, \dots, 37. \quad (6)$$

Assuming that the pusher plates move sinusoidally, the delay time t_m for each of these m segments is calculated as

$$t_m = \frac{\arcsin\left(\frac{x_{m+1} - 9.25 \text{ mm}}{9.25 \text{ mm}}\right) - \arcsin\left(\frac{x_m - 9.25 \text{ mm}}{9.25 \text{ mm}}\right)}{2\pi f}. \quad (7)$$

Finally, the position-dependent losses are weighted with the time factor t_m to calculate the average losses during one beat cycle

$$P_{avg} = f \cdot \sum_{m=0}^{36} (+P_{sum,fw}(x_m) \cdot t_m + P_{sum,bw}(x_{37-m}) \cdot t_{37-m}). \quad (8)$$

Based on this tool chain, the drive is optimized through a combination of analytical and numerical computations to achieve accurate results within the minimum computation time.

3. Optimization methods

The natural human heart weighs 400 g. Thus, evidently, the weight of the proposed drive has to be reduced. This weight reduction can be achieved by optimizing the drive's geometry and therefore by reducing, for example, its height or outer diameter. The Lorentz force Eq. (1) indicates that a drop in induction $B_n(x)$ caused by a reduced permanent-magnet volume or active wire lengths l results in lower producible forces. If the required forces $F(x)$ are similar, the current supply of the coils $I_n(x)$ has to be increased, thus increasing the resulting losses as well. However, 0 states that the electrical losses in the drive should be limited to 21 W to keep the temperature rise in the body below 1 °C. This statement has been proven by the temperature measurements in the total artificial heart called ReinHeart developed at RWTH Aachen University 0 during the Mock Loop tests. Therefore, a weight reduction in the drive can be achieved by optimizing its geometry. Although the allowable losses are only 20 W, the drive should be optimized in such a way that the required force is provided with resulting losses within the 10 W limit and minimal weight. A lower loss limit is required to allow for the peripheral components such as the battery, which should also be lightweight and small. This approach consequently reduces the drive dimensions as well.

3.1 Manual parameter variation

In the manual parameter variation, the influence of a limited number of objective variables on the resulting losses and weight of the drive is studied by varying each parameter at a fixed step width. For example, the outer radius is decreased in steps of 1 mm (Fig. 5). Evaluating the plots of the resulting weight against the losses establishes a hierarchical order, which indicates the best geometrical parameters to be varied. In this paper, the influence of the inner and outer radii, as well as the thickness of the coils, is presented and discussed. Finally, the optimization algorithm has to determine the best parameter combination for the optimum geometry of the drive while maintaining the maximum losses within the allowable range.

In Fig. 5, the outer and inner radii are decreased and increased, respectively, in steps of 1 mm. When the outer radius is reduced, a minimal weight of 495 g and resulting losses of 10.7 W are obtained. Meanwhile, when the inner radius is changed, the minimal weight only amounts to 582 g and the losses accumulate to 9.7 W. In this case, the achievable weight reduction is minimal. Therefore, the outer radius should be reduced first before increasing the inner radius.

In Fig. 6, the effect of coil thickness is investigated. The outer radius is reduced for coil thicknesses of 2 and 3 mm. The average coil radius is identical for both arrangements. However, comparison between the coils shows that the

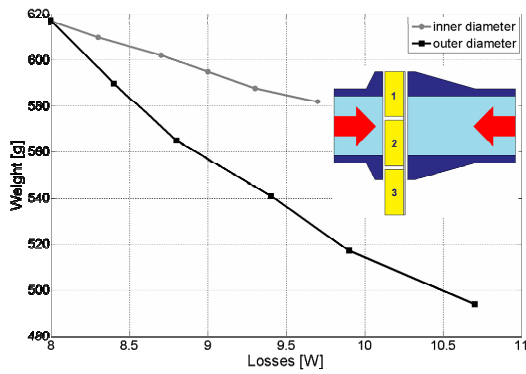


Fig. 5. Variations of inner and outer diameters.

thinner coil has an increased inner radius and a decreased outer radius. This approach increases the amount of air in the air gap. When the permanent magnets and pole shoes in the radial direction are increased, this amount is further reduced. Thus, the drive’s weight is reduced because the material density of the copper wire (8.92 g/cm³) is higher than those of the NdFeB magnets (7.4 g/cm³) and the Vacoflux (8.12 g/cm³) used for the pole shoes. In addition, the axial height of the coils is approximately twice those of the magnets and pole shoes. These conditions further decrease the weight. On the other hand, the coil’s resistance is increased because of the reduced cross section of the coils. Thus, the drive’s losses are decreased. This effect is partially compensated by the reduction of the leakage flux, which concentrates the flux density in the air gap more effectively. These complex correlations yield an intersection between the two curves when the losses and weight were 10.6 W and 500 g, respectively. When the outer radius is further decreased, the losses of a 2 mm thick coil variant are even lower than for the 3 mm thick coil variant.

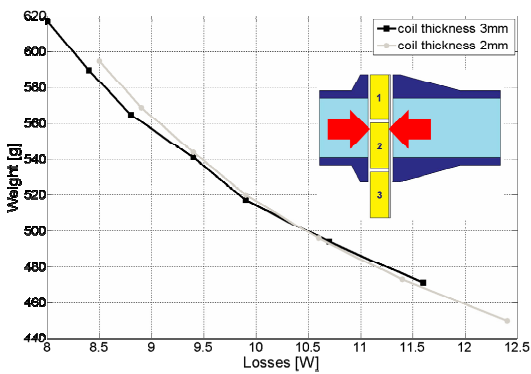


Fig. 6. Variation of coil thickness.

3.2 Differential evolution

DE is an evolutionary optimization algorithm [9]. First, the optimization parameters and their constraints are set. Then, a population of random models is created based on

these parameters. The quality of each model is determined using a predefined cost function

$$cf = a \cdot 10^{\left(\frac{|losses-10|}{10}\right)} + b \cdot 10^{\left(\frac{weight}{616}\right)} \tag{9}$$

Parameters *a* and *b* are initialized with a value between 0 and 1 such that the sum of *a* and *b* equals 1 to prioritize either the losses or the resulting weight during the optimization process. Therefore, theoretically, the best model has losses of 10 W and weighs 0 g. Based on the best model of this population, a new generation is created. After several iterations, as the algorithm converges, the optimum geometry of the drive is obtained without exceeding the allowable losses *L*. A cost function trigger was established to accelerate this process. Before evaluating the cost function, the resulting losses for all models are determined. Values that exceed the limit are multiplied by a factor of 10. Thus, the cost function value is significantly increased.

The results of the DE algorithm are presented in Fig. 7. For all plots, the *x*-axis represents the number of iterations, whereas the *y*-axis denotes the parameter indicated in the title of each plot. The convergence of the DE algorithm is shown in plot b by the mean distance to the cost function of each generated model. The mean distance is initially greater than 10⁵ and decreases quickly to a nearly constant value when the 28th iteration is reached. Thereafter, only slight differences are observed in the subsequent best models. In this plot, the cost functions of the best models are not shown for the first 11 iterations to emphasize the variations at the middle and end of the algorithm. Plots c and d illustrate the operation principle of the DE algorithm. In the applied cost function, the losses are prioritized. Initially, the losses exceed the given limit. When the cost function is triggered, the models are penalized and yield a high cost function value. Thus, the weight is reduced by changing the drive’s geometry, as indicated in plots e to i. As shown in plot b, the mean cost functions quickly reduced during the first few iterations. After the 12th iteration, the losses fall below the 10 W limit. As the weight is further reduced, the losses rise again until the global maximum of 9.99 W in the final model. Starting from the 20th iteration, the losses become constant but the weight is further reduced to its final value of 460 g.

4. Results

The final geometrical parameters and the resulting weights and losses for the two optimization methods and the prototype are listed in Table 1. The resulting losses for the parameter variation and DE were 9.94 and 9.99 W, respectively, which are close to the desired loss limit of 10 W. When compared to the losses of the prototype, these losses are larger by 2 W.

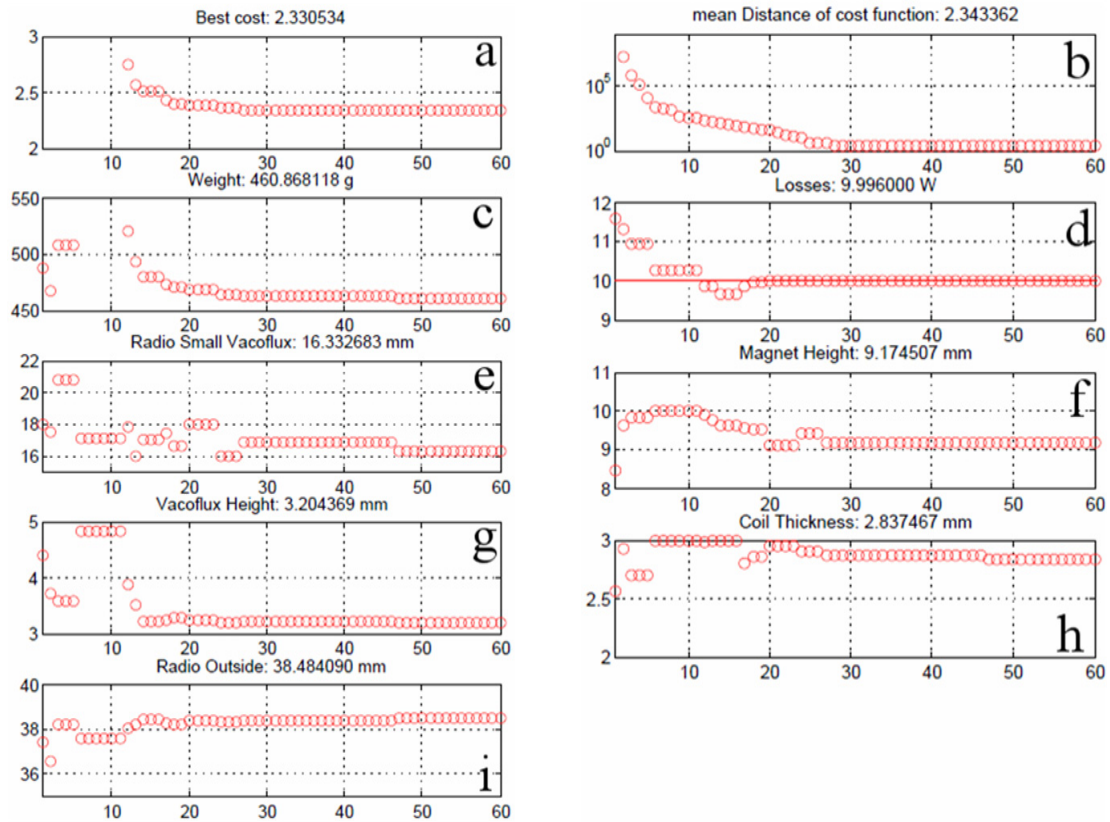


Fig. 8. Results of the DE algorithm.

Table 1. Comparison of the prototype and the optimized geometry

Parameter	Prototype	Variation calculations	Differential evolution
Weight	616 g	517 g	460 g
Losses	8 W	9.94 W	9.99 W
Inner radius	7 mm	8 mm	8 mm
Outer radius	42.5 mm	38.5 mm	38.45 mm
Maximum height	16.5 mm	16.5 mm	15.6 mm

The higher loss limit allowed for a weight reduction of 99 and 156 g for the parameter variation and DE, respectively. This variation is caused by the differences in the geometries obtained by the two methods. Although the inner (8 mm) and outer (38.5 and 38.45 mm) radii are nearly the same, the maximum height of the static drive part obtained by the DE algorithm is lower.

This and the other differences are shown in Fig. 7, which compares the geometrical parameters of the prototype (a) and those obtained by the parameter variation (b) and DE algorithm (c). The comparison between the axial dimensions of the magnets and the pole shoes of the different models shows that model c has a higher magnet height and lower pole shoe height. Its weight is reduced compared to that of model b because of the lower material density of the magnets and the reduced height of the static part. Model c also has a smaller average radius and coil

thickness values. Its electrical losses are higher because of the reduction of the active wire length l , whereas the balance between the induction $B_n(x)$ generated by the inner and outer permanent magnets is changed compared with that of model b. Therefore, higher weight reduction is achieved using the DE algorithm although the resulting losses are close to those obtained by parameter variation.

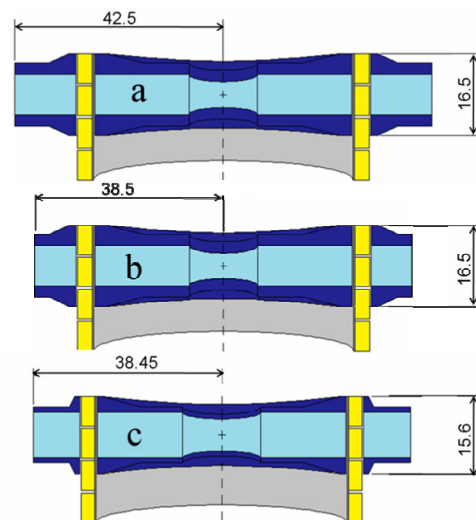


Fig. 7. Visualization of optimization results.

5. Conclusions

This paper has reported the optimization of the geometry of a drive for a pulsatile artificial heart. Two optimization approaches, namely, the parameter variation and DE algorithm, were discussed. Both rely on a calculation chain, which is a combination of FEM simulations, which determine the distribution of the magnetic induction, and analytical equations, which are used to calculate the resulting weight and the losses of the drive. The new drive geometries achieved by the two optimization approaches both had resulting losses close to the 10 W limit. However, the weight obtained by the DE approach was lower than that by parameter variation. In parameter variation, the geometrical parameters were varied with a fixed step width. This approach results in weight versus loss characteristics showing the sensitivity of each parameter. The disadvantage of this approach is that only one parameter can be actively changed. But the investigated geometrical parameters are all interdependent. In the DE algorithm, the computer models were created based on randomly chosen parameters, and therefore, their dependencies were considered. As the algorithm converged, the best possible results according to a predefined cost function were obtained. However, the effect of each parameter is not traceable, because they were initialized using random values. Furthermore, DE requires more computer models, compared with the parameter variation, because of its working principle.

Considering that the probability of nonconvergence increases with the increase in the parameters, a combination of both optimization approaches is advisable. After the sensitivities of some geometrical parameters are determined, the amount of parameters can then be reduced for the next DE optimization step, as well as the required number of models and, therefore, the computation time. DE proposed a coil thickness of 2.7 mm. Considering that the producible coil thickness depends on the available copper wire, an adjustment of the DE results is necessary to allow for manufacturing.

References

- [1] Abstracts from the 14th Congress of the International Society for Rotary Blood Pumps. *Artif. Organs*, 2006, 30(11): A27.
- [2] M. Lessmann, T. Finocchiaro, U. Steinseifer, T. Schmitz-Rode and K. Hameyer, "Concepts and designs of life support systems." *IET Science, Measurement & Technology* 2008, 2(6): 499-505.
- [3] www.vacuumschmelze.de, accessed February 2010
- [4] A. Pohlmann, M. Leßmann, T. Finocchiaro, A. Fritschi, T. Schmitz-Rode, and K. Hameyer, "Drive optimisation of a pulsatile Total Artificial Heart", in: *the XXI symposium electromagnetic phenomena in*

nonlinear circuits, EPNC 2010, pages 65-66, 2010.

- [5] www.iem.rwth-aachen.de, accessed May 2010
- [6] M. Yamaguchi, T. Yano, M. Karita, Y. Yamamoto, S. Yamada and H. Yamada, "Performance Test of a Linear Pulse Motor-Driven Artificial Heart", *IEEE Translation Journal in Japan*, Vol. 8, No. 2, February 1993.
- [7] A. Pohlmann, M. Leßmann, T. Finocchiaro, T. Schmitz-Rode, and K. Hameyer, "Numerical computation can save life: FEM simulations for the development of artificial hearts", *The 14th International Conference on Electromagnetic Field Computation*, CEFC, Chicago, USA, May 2010
- [8] K. V. Price, R. M. Storn and J. A. Lampinen, "Differential Evolution - A Practical Approach to Global Optimization", 1st ed., *Springer*, 2005.
- [9] U. K. Chakraborty, "Advances in Differential Evolution", *Springer*, 2008.
- [10] Hameyer, K., Belmans, R.: Numerical modelling and design of electrical machines and drives, Computational Mechanics Publications, *WIT Press*, Southampton 1999.



André Pohlmann He was born in Steinfurt, Germany, in 1982. He received his diploma degree in electrical engineering from RWTH Aachen University in October 2008. In December 2008, he started his doctoral studies at the Institute of Electrical Machines at RWTH Aachen University.

His field of research is on magnetic bearings and drives for artificial hearts.



Marc Leßmann He was born in 1977. He graduated in electrical engineering from RWTH Aachen University, Germany, in 2004. Currently, he is a Ph.D. student in the Institute of Electrical Machines at RWTH Aachen University. His research interests are high-speed machines, linear drives,

electromagnetic levitation techniques, and the development of life support systems such as total artificial hearts and ventricular assist devices.



Kay Hameyer Dr. Kay Hameyer received his M.Sc. degree in electrical engineering from the University of Hannover and his Ph.D. degree from Berlin University of Technology, Germany. After his academic studies, he worked with Robert Bosch GmbH in Stuttgart, Germany, as a Design

Engineer for permanent-magnet servo motors and vehicle board net components. Until 2004, Dr. Hameyer was a full Professor with KU Leuven, Belgium, where he taught Numerical Field Computations and Electrical Machines. Since 2004, he has been a full Professor and the Director of the Institute of Electrical Machines at RWTH Aachen University, Germany. In 2006, he was the Vice Dean of the aforementioned faculty, and from 2007 to 2009, he was the Dean of the Faculty of Electrical Engineering and Information Technology at RWTH Aachen University. His research interests are numerical field computation and optimization, the design and control of electrical machines, particularly permanent-magnet-excited machines, induction machines, and machine design using virtual reality methodology. For several years, Dr. Hameyer's work has been concerned with magnetic levitation for drive systems, magnetically excited audible noise in electrical machines, and the characterization of ferromagnetic materials. Dr. Hameyer is the author of more than 250 journal publications, more than 500 international conference publications, and 4 books. Dr. Hameyer is a member of VDE, senior member of IEEE, and fellow of IET.